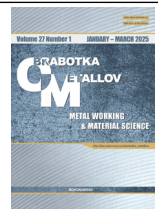




## Obrabotka metallov -

# Metal Working and Material Science

Journal homepage: [http://journals.nstu.ru/obrabotka\\_metallov](http://journals.nstu.ru/obrabotka_metallov)



## Designing the homogenization mechanism

*Yuriy Podgornyy*<sup>1, 2, a, \*</sup>, *Vadim Skeebea*<sup>1, b</sup>, *Tatyana Martynova*<sup>1, c</sup>, *Artur Sadykin*<sup>1, d</sup>,  
*Nikita Martyushev*<sup>3, e</sup>, *Dmitry Lobanov*<sup>4, f</sup>, *Arina Pelemeshko*<sup>1, g</sup>, *Andrey Popkov*<sup>1, h</sup>



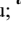

<sup>1</sup> Novosibirsk State Technical University, 20 Prospekt K. Marksa, Novosibirsk, 630073, Russian Federation





<sup>2</sup> Novosibirsk Technological Institute (branch) A.N. Kosygin Russian State University (Technologies. Design. Art), 35 Krasny prospekt (5 Potaninskayast.), Novosibirsk, 630099, Russian Federation





<sup>3</sup> National Research Tomsk Polytechnic University, 30 Lenin Avenue, Tomsk, 634050, Russian Federation

<sup>4</sup> I. N. Ulianov Chuvash State University, 15 Moskovsky Prospekt, Cheboksary, 428015, Russian Federation

<sup>a</sup>  <https://orcid.org/0000-0002-1664-5351>,  [pjui@mail.ru](mailto:pjui@mail.ru); <sup>b</sup>  <https://orcid.org/0000-0002-8242-2295>,  [skeebea\\_vadim@mail.ru](mailto:skeebea_vadim@mail.ru);

<sup>c</sup>  <https://orcid.org/0000-0002-5811-5519>,  [martynova@corp.nstu.ru](mailto:martynova@corp.nstu.ru); <sup>d</sup>  <https://orcid.org/0009-0002-2061-650X>,  [artur060779@gmail.com](mailto:artur060779@gmail.com);

<sup>e</sup>  <https://orcid.org/0000-0003-0620-9561>,  [martjushev@tpu.ru](mailto:martjushev@tpu.ru); <sup>f</sup>  <https://orcid.org/0000-0002-4273-5107>,  [lobanovdv@list.ru](mailto:lobanovdv@list.ru);

<sup>g</sup>  <https://orcid.org/0009-0004-5916-6782>,  [pyatkova.arina@gmail.com](mailto:pyatkova.arina@gmail.com); <sup>h</sup>  <https://orcid.org/0009-0006-5587-9990>,  [andrey.popkov.2013@mail.ru](mailto:andrey.popkov.2013@mail.ru)

### ARTICLE INFO

#### Article history:

Received: 14 December 2024

Revised: 09 January 2025

Accepted: 31 January 2025

Available online: 15 March 2025

#### Keywords:

Homogenization  
 Cycle diagram of operation  
 Kinematic scheme  
 Cam mechanism  
 Pusher  
 Roller  
 Speed  
 Accelerations  
 Motions  
 Cam profile

#### Funding

This study was supported by a NSTU grant (project No. TP-PTM-1\_25).

#### Acknowledgements

The research was carried out at the equipment of the Engineering Center "Design and Production of High-Tech Equipment".

### ABSTRACT

**Introduction.** The primary goal of food processing equipment manufacturing is to create highly efficient process equipment that can increase labor productivity while reducing energy costs. Improving existing and creating new high-performance equipment for food production is one of the main trends in the development of modern mechanical engineering. The term "homogenization" literally means "increasing uniformity". In the context of emulsions, homogenization refers to the process of treating emulsions, which leads to the fragmentation of the dispersed phase. Homogenization is the process of grinding liquid or mashed foods by passing it at high speed and pressure through narrow annular slots. The authors propose to use cam-type mechanisms for homogenization. Cam-type mechanisms allow for a more efficient allocation of the time for the product suction and injection. The homogenization process benefits from the potential to reduce the speed during product injection. **The purpose of the work** is to reduce power consumption during homogenization. **The research methods** are based on the theory of machines and mechanisms. These methods enabled developing a methodology for synthesizing the homogenizer drive mechanism and designing a machine that ensures its operation in accordance with the proposed cycle diagram. **Results and discussion.** The synthesis of mechanisms is executed with consideration for the workload, which was calculated for existing domestic machines in the production of processed cheese. Thus, with a given production capacity of 550 l/h and a plunger diameter of 28 mm, the technological force is  $F = 12315$  N. In accordance with the authors' proposals, the design of the homogenizer is modified by introducing cam mechanisms. In the design of this drive, a novel cycle diagram is proposed, enabling an increase in product injection time and a reduction in suction time. According to the novel cycle diagram,  $280^\circ$  is proposed for product injection and  $80^\circ$  for suction. In this case, the power on the drive shaft is equal to  $P = 2.5$  kW instead of 3.5 kW for the existing design, driven by a crank mechanism. The power consumption is decreased by 26 %.

**For citation:** Podgornyy Y.I., Skeebea V.Y., Martynova T.G., Sadykin A.V., Martyushev N.V., Lobanov D.V., Pelemeshko A.K., Popkov A.S. Designing the homogenization mechanism. *Obrabotka metallov (tehnologiya, oborudovanie, instrumenty) = Metal Working and Material Science*, 2025, vol. 27, no. 1, pp. 129–142. DOI: 10.17212/1994-6309-2025-27.1-129-142. (In Russian).

#### \* Corresponding author

*Podgornyy Yuriy I.*, D.Sc. (Engineering), Professor  
 Novosibirsk State Technical University,  
 20 Prospekt K. Marksa,  
 630073, Novosibirsk, Russian Federation  
 Tel: +7 383 346-17-79, e-mail: [pjui@mail.ru](mailto:pjui@mail.ru)

## Introduction

The primary goal of food processing equipment manufacturing is to create highly efficient processing equipment that can increase labor productivity while reducing energy costs. Homogenization machines are among the many types of process equipment used in food industry enterprises [1–9]. Among the many critical features of contemporary processing machines, the equipment's performance, technical condition, and product quality are the most important [10–19].

Enhancing existing and developing novel, high-performance equipment for food production is a key trend in modern mechanical engineering. As dynamic stresses and operating speeds increase, more stringent demands are placed on the design of individual components and assemblies, such as the drives that ensure intermittent motion of the machine's working parts [7, 12–14, 16–22]. A significant requirement for modern machines is that the follower movements accurately correspond to a specific motion profile. Therefore, the use of cam-type mechanisms is proposed for food processing machines, as they allow for efficient control of the timing for product suction and injection. The motion profiles of cam mechanisms can be synthesized in a wide variety of ways, making them easily adaptable to the kinematic and dynamic requirements specified by the developer. Furthermore, the technology for obtaining the required cam profile has been firmly established ensuring accurate follower motion [23–35]. The homogenization process can benefit from the ability to reduce speed during product injection [36, 37].

The term “homogenization” literally means “increasing uniformity”. In the context of emulsions, homogenization refers to the process of treating emulsions that results in the fragmentation of the dispersed phase. More specifically, homogenization is the process of grinding liquid or mashed foods by passing them at high speed and pressure through narrow annular slots. The homogenization process is widely used in the food industry, particularly in the dairy industry, for example, in the manufacture of processed cheese.

Processed cheese is a food product that has undergone melting and homogeneous distribution of its components. It is produced from specific mixtures formulated with a clear, specific recipe that details the ingredients: the components of milk, cream, butter, cheeses, melting salts, stabilizers, as well as flavors and additives. The technology for manufacturing processed cheese includes several stages. First, the cheese or cottage cheese is crushed and mixed. The mixture is then melted and emulsified, and special additives that aid in achieving the product's desired consistency and texture, such as structurizers or emulsifying salts, may be used.

According to analysis, homogenizer designs most frequently utilize crank mechanisms. Preliminary research [1–7, 12, 13, 36] suggests that laminar flow invariably results in a threefold increase in the degree of dispersion of fat globules compared to turbulent flow. Cheese is produced using specialized machines called *homogenizing machines*, and their indicator diagrams can be viewed in detail in [36]. The constituent elements of the diagram include the moments of product suction and injection through the annular slot. Product suction occurs at a pressure lower than atmospheric one, while injection through an annular slot occurs at a pressure of 20 MPa or higher.

In conventional designs, the operation of the crank mechanism is divided into two sections: the first section is *suction*, which takes up half the distance traveled by the crank, and the second section provides *injection*, taking the second half of the distance. The disadvantage of such designs is their high power consumption. Therefore, we believe that replacing the crank mechanism with a cam mechanism is a promising, relevant, and timely task.

**The purpose of the work** is to reduce power consumption during product homogenization

**To achieve this purpose, the following tasks were addressed:**

- the technological load during homogenization was determined;
- the feasibility of replacing the crank mechanism with a cam mechanism was analyzed;
- the necessary parameters for synthesizing of the cam pair were selected, and the synthesis was performed;
- a novel cycle diagram of the device operation was proposed;

- the resistance forces torque has been determined, both for each camshaft individually and for the total torque;
- the power required for homogenization with the proposed new drive was determined.

### Research methodology

The first step in this research involved determining the technological load during the homogenization process in processed cheese manufacturing. According to [37], the operating pressure in the cylinder cavity at the moment of liquid injection is 20 MPa. With a plunger diameter of  $d = 28$  mm and a production capacity of 550 L/h, and a main shaft rotation speed of  $n = 180 \text{ min}^{-1}$ , the required force exerted by the plunger on the liquid in the homogenizing head's passage section was determined to be  $F = 12,315$  N. Kinetostatic analysis of this mechanism indicated that the required power consumption for this case is 3.8 kW.

The details of the cam-driven homogenizer design proposed by the authors are presented below. Fig. 1 illustrates the locations of the drive cams and pushers driving the plungers. Functionally, all other elements operate in the same manner as in drives with crank mechanisms. Detailed information about the design of the homogenizer can be found in [37].

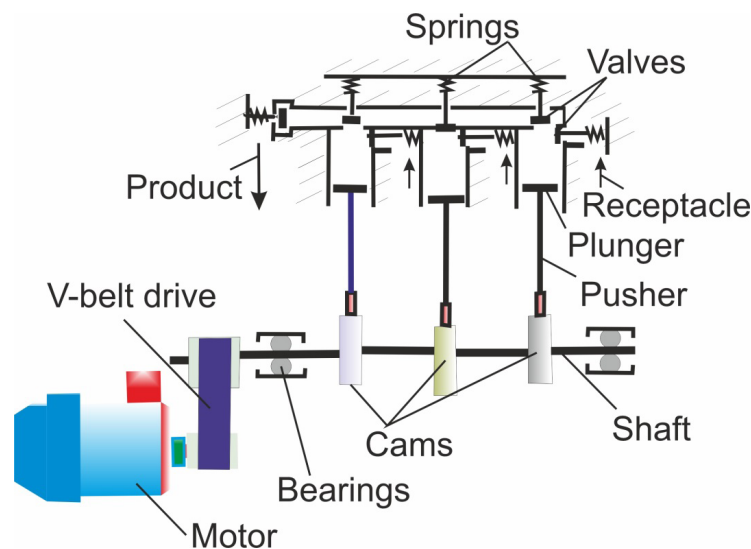


Fig. 1. The proposed design of a cam-driven homogenizer

Numerous motion laws are applicable to cam mechanisms in mechanics. To select an motion law, we propose considering three common types:

- simple harmonic motion law;
- double harmonic motion law;
- cycloidal motion laws [7, 12, 13–27, 31–35, 38–41].

The design scheme for the cam mechanism is shown in Fig. 2. The following parameters were considered as variables: profile angles  $\beta$ ; phase angles of motion for ascent and descent –  $\varphi_1, \varphi_2, \varphi_3, \varphi_4$ ; the maximum displacement of the pusher is  $S_{max}$ ; current value of the cam rotation angle  $\varphi$ . Due to the fact that all calculations were performed using a mathematical software package, the following notation was adopted for clarity: displacement  $s(\varphi)$ ; velocity  $v_f(\varphi)$ ; acceleration  $a_f(\varphi)$ ; and torques on the working shaft  $M_1(\varphi)$ ,  $M_2(\varphi)$ ,  $M_3(\varphi)$ , corresponding to the three cams involved in the design; coefficients for the harmonic motion law  $k_1 = \frac{S_{max}}{2}$ ,  $k_3 = -S_{max} \frac{6}{\varphi_3^2}$ ; workload forces during product injection and suction,  $F_1, F_2$ , which were assumed to be  $F_1 = 12,315$  N and  $F_2 = 2,500$  N, respectively.

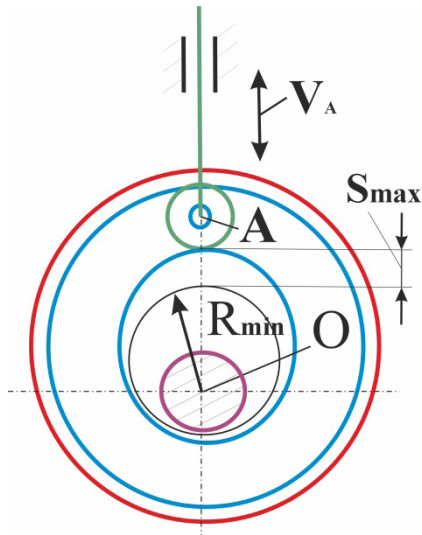


Fig. 2. Cam mechanism of the homogenizer

The results of this study indicated that simple harmonic motion law is the most suitable one, as its maximum velocity values were 25 % and 30 % lower than those of double harmonic and cycloidal motion laws, respectively. The analytical expression for simple harmonic motion law is given by:

$$s(\phi) = \frac{S_{\max}}{2} \cdot \left( 1 - \cos\left(\pi \cdot \frac{\phi}{\beta}\right) \right), \quad (1)$$

The kinematic characteristics for simple harmonic motion law were calculated using the *Mathcad* software package, with the listing shown in Fig. 3.

$$a(\varphi) := \begin{cases} k_1 \cdot \frac{\pi}{\phi_1} \cdot \cos\left(\pi \cdot \frac{\phi}{\phi_1}\right) & \text{if } 0 \leq \phi \leq \phi_1 \\ 0 & \text{if } \phi_1 \leq \phi \leq \phi_1 + \phi_2 \\ k_3 \cdot \left[ 1 - 2 \cdot \frac{\phi - (\phi_1 + \phi_2)}{\phi_3} \right] & \text{if } \phi_1 + \phi_2 \leq \phi \leq \phi_1 + \phi_2 + \phi_3 \\ 0 & \text{if } \phi_1 + \phi_2 + \phi_3 \leq \phi \leq 360 \text{ deg,} \end{cases} \quad (2)$$

The speed is defined as:

$$v(\varphi) = \begin{cases} \left[ \left( -k_1 \cdot \frac{\pi}{\phi_1} \right) \cdot \sin\left(\frac{\pi \cdot \phi}{\phi_1}\right) \right] & \text{if } 0 \leq \phi \leq \phi_1 \\ 0 & \text{if } \phi_1 \leq \phi \leq \phi_2 + \phi_1 \\ k_3 \cdot \left[ \phi - (\phi_1 + \phi_2) \right] \cdot \left[ 1 - \frac{\phi - (\phi_1 + \phi_2)}{\phi_3} \right] & \text{if } \phi_1 + \phi_2 \leq \phi \leq \phi_1 + \phi_2 + \phi_3 \\ 0 & \text{if } \phi_1 + \phi_2 + \phi_3 \leq \phi \leq 360 \text{ deg,} \end{cases} \quad (3)$$

Fig. 3. Listing of a program for determining kinematic characteristics

Displacement was calculated as the integral function of the velocities, using Equation (3):

$$s(\varphi) = \int_0^{\phi} v(\phi) \cdot d\phi. \quad (4)$$

The torque acting on the first cam was determined using a program developed within the mathematical software package. The program listing is shown in Fig. 4.

$$v(\varphi) = \begin{cases} \left[ \left( k_1 \cdot \frac{\pi}{\phi_1} \right) \cdot \sin \left( \pi \cdot \frac{\phi}{\phi_1} \right) \cdot F_1 \right] & \text{if } 0 \leq \phi \leq \phi_1 \\ 0 & \text{if } \phi \leq \phi \leq \phi_1 + \phi_2 \\ \left[ k_3 \cdot \phi - \phi_1 + \phi_2 \cdot \left[ 1 - \frac{\phi - \phi_1 + \phi_2}{\phi_3} \right] \right] \cdot F_2 & \text{if } \phi_1 + \phi_2 \leq \phi \leq \phi_1 + \phi_2 + \phi_3 \\ 0 & \text{if } (\phi_1 + \phi_2 + \phi_3) \leq \phi \leq 360 \text{ deg} \end{cases} \quad (5)$$

Fig. 4. Listing of the program for determining the torque on the cam shaft

The torques for the second and third cams can be expressed as follows:

$$\begin{aligned} M_2(\phi) &= M_1(\phi + \psi_2), \\ M_3(\phi) &= M_1(\phi + \psi_3), \end{aligned} \quad (6)$$

where  $M_2$  and  $M_3$  are the torques for the second and third cams;  $\psi_1$ ,  $\psi_2$  are the phase displacement angles for the cams on the drive shaft.

The torques on the drive shaft (cam) were determined based on the phase shift magnitudes of the angles  $\psi_i$  and profile angles  $\beta_i$ . The total torque  $M_c$  on the drive shaft was determined as the sum of the component torques  $M_i$ , of which there are three in this case:

$$M_c = \sum_{i=1}^3 M_i. \quad (7)$$

The power consumption applied to the drive shaft can be expressed as [34]:

$$P = M_c \max \omega, \quad (8)$$

where  $M_{cmax}$  is the maximum value of the total torque.

The profile angles  $\beta$  were determined iteratively using the programs shown in Figs. 3 and 5. As a result, by identifying the minimum velocity value from the family of curves, we selected simple harmonic motion law with profile angles  $\beta_1 = 280^\circ$  and  $\beta_2 = 80^\circ$  and initiated the design of the cam mechanism according to the specified parameters [12].

Furthermore, the pressure angles were determined using the following Equation:

$$\delta(\phi) = a \tan \left( \frac{v(\phi) + e1}{sh + s(\phi)} \right). \quad (9)$$

To achieve this, it was necessary to find the cam's minimum radius,  $R_{min}$ . A graph was constructed in  $v(s)$  coordinates using the calculated position functions  $s(\varphi)$  and velocity analogs  $v(\varphi)$  (Fig. 6) during the ascent and descent phases. The only difference in this process was the use of numerical velocity values. The resulting scheme is shown in Fig. 7. The velocity vectors are indicated by points from  $A_0$  to  $A_s$ . The ascent phase is represented by points from  $A_0$  to  $A_p$ , and the descent phase, from  $A_s$  to  $A_s$ . The minimum cam radius vector was determined to be  $R_{min} = 90$  mm.

The next step in determining the design parameters of the mechanism is to determine the roller radius. This can be found using an algorithm that calculates the radii of curvature for the cam profile based on its rotation angle. The curvature radius values,  $\rho_{cur}$ , can be calculated using a general formula applicable to any cam type [23]:

$$\rho_{cur} = \frac{\left[ \rho^2 + \left( \frac{d\rho}{d\beta} \right)^2 \right]^{3/2}}{\rho^2 + 2 \left( \frac{d\rho}{d\beta} \right)^2 - \rho \frac{d^2\rho}{d\beta^2}}, \quad (10)$$

where  $p$  is the radius vector of the theoretical profile;  $\beta$  is the profile angle.

$i := 0.5..180$  – Discrete angle values

$f_{1i1} := i1 \cdot \frac{\pi}{180}$  – Conversion of angles from degrees to radians in section 1

$v_{1i1} := v(f_{1i1})$  – Velocity analog in section 1

$v_{1\max} := \max(v1)$  – Maximum velocity analog in section 1

$v_{1\max} = 0.01$  – Velocity analog value in section 1

$v_{1,90} = 0.019$  – Maximum velocity analog value in section 1 at  $\varphi = 90^\circ$

$s_{1i1} := s(f_{1i1})$  – Displacement of the driven link in section 1

$s_{1\max} := s(90 \text{ deg})$  – Maximum displacement of the driven link in section 1

$s_{1\max} = 0.015$  – Maximum displacement value of the driven link in section 1

$\varepsilon_2 := a \tan\left(\frac{s_{3\max} - s_{1\max}}{v_{1\max} - v_{3\max}}\right)$  – Angle value in section 2

$\varepsilon_3 := \left(\frac{\pi}{2}\right) - \delta\text{dop} + \varepsilon_2$  – Angle value in section 3

$\varepsilon_1 := 2 \cdot \delta\text{dop}$  – Angle value in section 1

$e_1 := l_{31} \cdot \sin(\delta\text{dop}) - (v_{1\max})$  – Eccentricity in section 1

$s_h := l_{31} \cdot \cos(\delta\text{dop}) - s_{1\max}$  – Roller center displacement

$s_h = 0.014$  – Roller center displacement value

$i_3 := 180..360$  – Discrete angle values

$f_{3i3} := i3 \cdot \frac{\pi}{180}$  – Conversion of angles from degrees to radians in section 3

$v_{3i3} := |v(f_{3i3})|$  – Velocity analog in section 3

$v_{3\max} := -\max(v3)$  – Velocity analog value in section 3

$v_{3\max} = -0.014$  – Maximum velocity analog value in section 3

$v_{3,70} = 0.014$  – Velocity analog value in section 3 at  $\varphi = 70^\circ$

$s_{3i3} := s(f_{3i3})$  – Displacement of the driven link in section 3

$s_{3\max} := s(270 \text{ deg})$  – Maximum displacement of the driven link in section 3

$s_{3\max} = 0.015$  – Maximum displacement value of the driven link in section 3

$l_{34} := \frac{|v_{1\max} - v_{3\max}|}{\cos(\varepsilon_2)}$  – Difference between maximum velocity values in section 3–1 of the profile

$\varepsilon_4 := \left(\frac{\pi}{2}\right) - \delta\text{dop} - \varepsilon_2$  – Angle value in section 4

$l_{31} := l_{34} \cdot \frac{\sin(\varepsilon_4)}{\sin(\varepsilon_1)}$  – Difference between maximum velocity values in section 3–1 of the profile

$l_{31} = 0.033$  – Difference value between velocity analogs in section 3–1

Fig. 5. Listing of a program for determining pressure angles  $\delta$

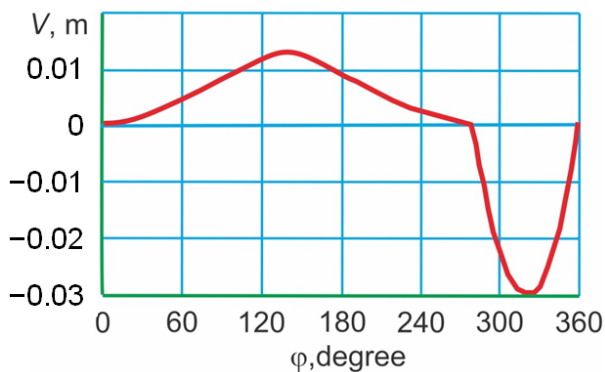


Fig. 6. Graph of analog speeds of the cam mechanism's roller center



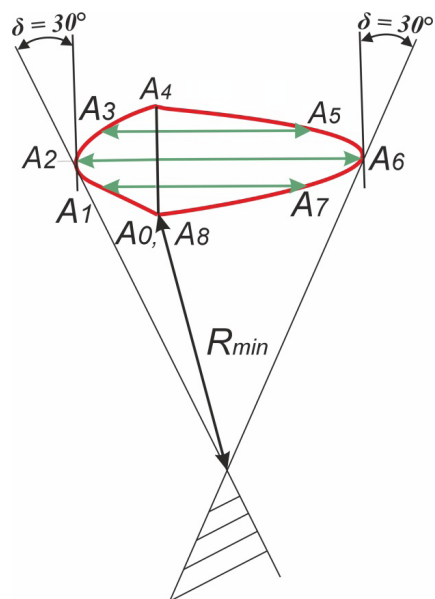


Fig. 7. Diagram of determining the minimum radius vector for a mechanism with a pusher

When writing a program to determine the minimum curvature radius, it is necessary to consider the interpolation of the radius vector values for the displacements of the cam mechanism's roller center [12].

A listing of the program for determining the cam surface curvature is shown in Fig. 8.

$k := 0..360 \text{ deg}$  – Discrete angle values

$f_k := k \cdot \frac{\pi}{180}$  – Conversion of angle from degrees to radians

$v_{xk} := \beta(f_k)$  – Velocity analog in the  $k^{\text{th}}$  section along the  $x$  – axis

$v_{yk} := \rho(f_k)$  – Velocity analog in the  $k^{\text{th}}$  section along the  $y$  – axis

$R := \text{cspline}(v_x, v_y)$  – Spline processing of the velocity analog value array

$f_{it}(x) := \text{interp}(R, v_x, v_y)$  – Interpolation of the radius vector  $R$  array value

$df_{it}(x) := \frac{d}{dx} f_{it}(x)$  – First derivative of the  $f_{it}(x)$  function

$d2f_{it}(x) := \frac{d^2}{dx^2} f_{it}(x)$  – Second derivative of the  $f_{it}(x)$  function

$\rho_{cur}(x) := \frac{(f_{it}(x)^2 + df_{it}(x)^2)^{1.5}}{f_{it}(x)^2 + 2 \cdot df_{it}(x)^2 - d2f_{it}(x) \cdot f_{it}(x)}$  – Formula defining the radii of curvature

of the cam profile

$i_1 := 0..280 \text{ deg}$  – Discrete angle values

$f_{1i1} := i_1 \cdot \frac{\pi}{180}$  – Conversion of angle from degrees to radians

$\rho_{cur1i1} := \rho_{cur}(f_{1i1})$  – Radius of curvature of the cam profile in section 1

$\min(\rho_{cur1}) = 0.03$  – Minimum radius of curvature of the profile in section 1

Fig. 8. Listing of a program for determining the curvature of the cam surface

## Results and Discussions

Analyzing the obtained power consumption values, we concluded that it is 3.8 kW for a crank mechanism. For a simple harmonic motion law, it is 3.8 kW; for cycloidal and double harmonic motion law, it is 4.5 kW and 4.3 kW, respectively. These values were calculated at equal profile angles  $\beta = 180^\circ$ . The authors suggest that the new cycle diagram of the cam drive operation should provide a significant reduction in torque for

the follower and, consequently, lead to a decrease in power consumption. Using the calculation algorithms shown in Figs. 4, 5, and 8, and setting the phase angles for suction and injection in  $20^\circ$  increments, we obtained values for the pressure angles. One calculation option is presented below.

*Option 1.* The phase angle for the injection and suction moment is  $180^\circ$ . The graphs for this option are shown in Fig. 9.

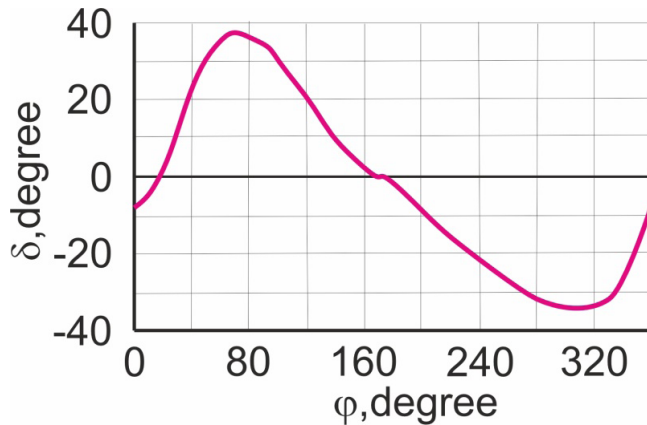


Fig. 9. Graph of pressure angle variations

As can be seen from the graph, the pressure angle values at  $70^\circ$  and  $310^\circ$  exceed acceptable limits. Therefore, this option is not viable for the homogenizer design. Subsequently, five more options were proposed (Table 1). Of the family of curves presented in Table 1, only one satisfies the requirement: the pressure angles throughout a full rotation ( $360^\circ$ ) do not exceed the permissible value of  $30^\circ$ .

This curve has phase angles of  $280^\circ$  for the injection period and  $80^\circ$  for the suction period. Subsequently, using these parameters as a basis, we initiated the cam synthesis. For preliminary calculations during synthesis, the following cycle diagram parameters were used:  $80^\circ$  was allocated for suction, and  $280^\circ$  of the full cam rotation was allocated for liquid injection. Formula (5) was used to determine the torque on the cam. The numerical values of the forces at the injection and suction moments were assumed to be  $F_1 = 12,315$  N and  $F_2 = 2,500$  N, respectively. For one variant, graphs of the torques at phase displacement angles  $\psi_1 = 170^\circ$  and  $\psi_2 = 340^\circ$  are shown in Fig. 10. The total torque acting on the drive shaft is indicated in purple. The data for the remaining options are summarized in Table 2.

Only *Option 5* (also depicted in Fig. 10) exhibits the lowest total torque value on the camshaft, as evident from the table above.

Following a thorough analysis of the available options, the cam mechanism synthesis can begin with the following specifications:  $280^\circ$  and  $80^\circ$  for injection and suction, based on the cycle diagram; a pusher stroke of 30 mm; and a minimum curvature radius of 90 mm.

Table 1

Options for investigating pressure angles

| No. | Phase angles                  |                                 | Values of maximum pressure angles, degrees |
|-----|-------------------------------|---------------------------------|--|
|     | $\varphi$ , degrees (suction) | $\varphi$ , degrees (injection) |  |
| 1   | 200                           | 160                             | 32   |
| 2   | 220                           | 140                             | 33   |
| 3   | 240                           | 120                             | 32   |
| 4   | 260                           | 100                             | 31   |
| 5   | 280                           | 80                              | 25   |



Torque values on the drive shaft

| No. | Phase angles                  |                                 | Torque values on the drive shaft, N·m |
|-----|-------------------------------|---------------------------------|---------------------------------------|
|     | $\varphi$ , degrees (suction) | $\varphi$ , degrees (injection) |                                       |
| 1   | 120                           | 240                             | 185                                   |
| 2   | 140                           | 260                             | 186                                   |
| 3   | 160                           | 280                             | 185                                   |
| 4   | 180                           | 300                             | 186                                   |
| 5   | 170                           | 340                             | 137                                   |

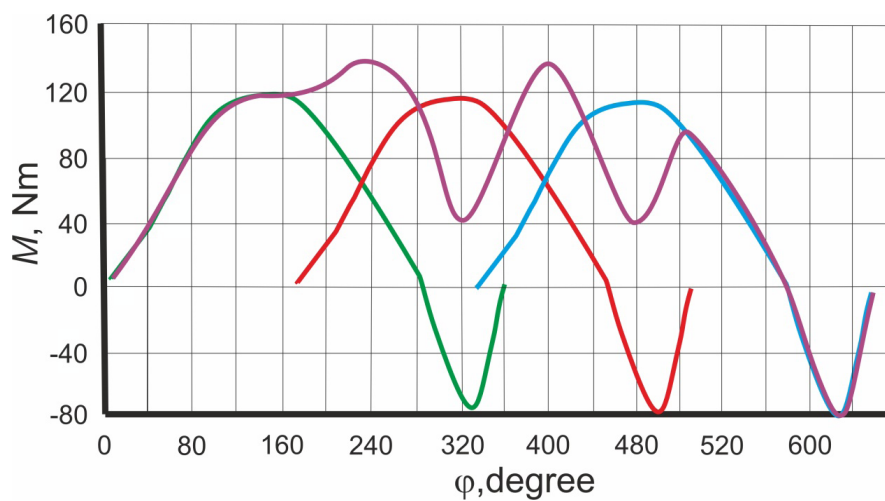
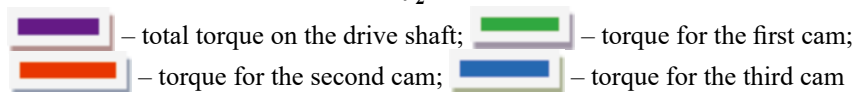
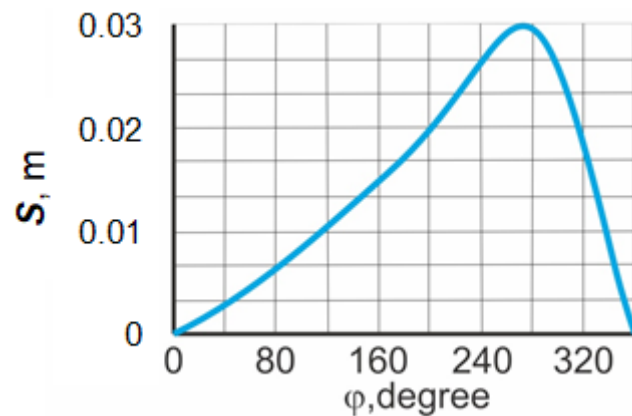


Fig. 10. Graphs of torques with a phase displacement angle  $\psi_1 = 170$  and  $\psi_2 = 340$ :



The displacements and velocities were determined according to the listing in Fig. 3 and Equation 4. The displacements are shown in Fig. 11, and the cam profile is shown in Fig. 12.

Fig. 11. Graph of displacement variations



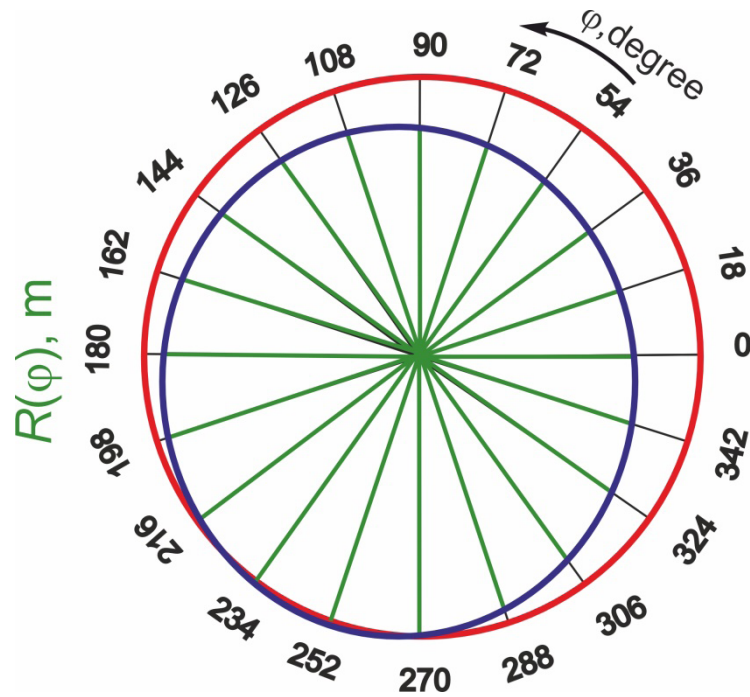


Fig. 12. Cam profile

## Conclusion

The primary objective of this research was to reduce the power consumption of the homogenizer.

Using the analytical relationships (1–4) and setting specific numerical values for the cam mechanism parameters, we selected the most efficient pusher motion law in the form of a simple harmonic curve. This law exhibits the minimum velocity values among the considered family of mathematical curves. The amplitude values of the velocity analogs were 0.012 m in the positive region and  $-0.03$  m in the negative region. The pressure angles for this curve do not exceed the permissible value of  $\delta = 30^\circ$  across the entire studied angle range. The presented torque dependencies on the drive shaft indicate the appropriateness of setting their displacement angles to  $\psi_1 = 170^\circ$  and  $\psi_2 = 340^\circ$ . In this configuration, the total torque was 137 N·m, and the power on the drive shaft was  $P = 2.5$  kW, compared to 3.8 kW for the existing design driven by a crank mechanism. This represents a 34 % decrease in power consumption.

## References

1. Inguva P., Grasselli S., Heng P.W.S. High pressure homogenization – An update on its usage and understanding. *Chemical Engineering Research and Design*, 2024, vol. 202, pp. 284–302. DOI: 10.1016/j.cherd.2023.12.026.
2. Chen X., Liang L., Xu X. Advances in converting of meat protein into functional ingredient via engineering modification of high pressure homogenization. *Trends in Food Science & Technology*, 2020, vol. 106, pp. 12–29. DOI: 10.1016/j.tifs.2020.09.032.
3. Chevalier-Lucia D., Picart-Palmade L. High-pressure homogenization in food processing. *Green food processing techniques*. Ed. by F. Chemat, E. Vorobiev. Elsevier, Academic Press, 2019, pp. 139–157. DOI: 10.1016/B978-0-12-815353-6.00005-7.
4. Luo D., Fan J., Jin M., Zhang X., Wang J., Rao H., Xue W. The influence mechanism of pH and polyphenol structures on the formation, structure, and digestibility of pea starch-polyphenol complexes via high-pressure homogenization. *Food Research International*, 2024, vol. 194, p. 114913. DOI: 10.1016/j.foodres.2024.114913.
5. Mehmood T., Ahmad A., Ahmed A., Ahmed Z. Optimization of olive oil based O/W nanoemulsions prepared through ultrasonic homogenization: a response surface methodology approach. *Food Chemistry*, 2017, vol. 229, pp. 790–796. DOI: 10.1016/j.foodchem.2017.03.023.
6. Ma Z., Zhao Y., Khalid N., Shu G., Neves M.A., Kobayashi I., Nakajima M. Comparative study of oil-in-water emulsions encapsulating fucoxanthin formulated by microchannel emulsification and high-pressure homogenization. *Food Hydrocolloids*, 2020, vol. 108, p. 105977. DOI: 10.1016/j.foodhyd.2020.105977.



7. Podgornyj Y.I., Skeebe V.Y., Martynova T.G. *Tekhnologicheskoe oborudovanie: raschet i proektirovanie* [Technological equipment: calculation and design]. Novosibirsk, NSTU Publ., 2024. 107 p. ISBN 978-5-7782-5308-7.
8. Tenorio-Garcia E., Araiza-Calahorra A., Simone E., Sarkar A. Recent advances in design and stability of double emulsions: trends in Pickering stabilization. *Food Hydrocolloids*, 2022, vol. 128, p. 107601. DOI: 10.1016/j.foodhyd.2022.107601.
9. Costa A.L.R., Gomes A., Andrade C.C.P., Cunha R.L. Emulsifier functionality and process engineering: progress and challenges. *Food Hydrocolloids*, 2017, vol. 68, pp. 69–80. DOI: 10.1016/j.foodhyd.2016.10.012.
10. Skeebe V.Yu., Ivancivsky V.V. *Gibridnoe metalloobratyvayushchee oborudovanie: povyshenie effektivnosti tekhnologicheskogo protsessa obrabotki detalei pri integratsii poverkhnostnoi zakalki i abrazivnogo shlifovaniya* [Hybrid metal working equipment: improving the effectiveness of the details processing under the integration of surface quenching and abrasive grinding]. Novosibirsk, NSTU Publ., 2018. 312 p. ISBN 978-5-7782-3690-5.
11. Podgornyj Yu.I., Skeebe V.Yu., Kirillov A.V., Pushnin V.N., Erokhin I.A., Kornev D.Yu. *Modelirovanie nesushchikh sistem tekhnologicheskikh mashin* [Modeling of the technological machines support systems]. *Obrabotka metallov (tekhnologiya, oborudovanie, instrumenty) = Metal Working and Material Science*, 2014, no. 2 (63), pp. 91–99.
12. Podgornyj Yu.I., Skeebe V.Yu., Martynova T.G., Maksimchuk O.V. *Issledovanie i vybor parametrov pri proektirovanii tekhnologicheskikh mashin* [Analysis and choice of parameters in designing technological machines]. Novosibirsk, NSTU Publ., 2020. 260 p. ISBN 978-5-7782-4177-0.
13. Podgornyj Yu.I., Martynova T.G., Skeebe V.Yu. *Sintez tekhnologicheskikh mashin. Raschet i konstruirovaniye* [Synthesis of technological machines. calculation and design]. Novosibirsk, NSTU Publ., 2023. 240 p. ISBN 978-5-7782-4912-7. DOI: 10.17212/978-5-7782-4912-7.
14. Flores P., Souto A.P., Marques F. The first fifty years of the mechanism and machine theory: standing back and looking forward. *Mechanism and Machine Theory*, 2018, vol. 125, pp. 8–20. DOI: 10.1016/j.mechmachtheory.2017.11.017.
15. Chen K., Wang M., Huo X., Wang P., Sun T. Topology and dimension synchronous optimization design of 5-DoF parallel robots for in-situ machining of large-scale steel components. *Mechanism and Machine Theory*, 2023, vol. 179, p. 105105. DOI: 10.1016/j.mechmachtheory.2022.105105.
16. Eckhardt H.D. *Kinematic design of machines and mechanisms*. 1st ed. New York, McGraw-Hill, 1998. 620 p. ISBN 0070189536. ISBN 978-0070189539.
17. Erdman A.G., Sandor G.N. *Mechanism design: analysis and synthesis*. 4th ed. Upper Saddle River, NJ, Pearson, 2001. 688 p. ISBN 0130408727. ISBN 978-0130408723.
18. Hsieh J.-F. Design and analysis of indexing cam mechanism with parallel axes. *Mechanism and Machine Theory*, 2014, vol. 81, pp. 155–165. DOI: 10.1016/j.mechmachtheory.2014.07.004.
19. Zhu B., Zhang X., Zhang H., Liang J., Zang H., Li H., Wang R. Design of compliant mechanisms using continuum topology optimization: a review. *Mechanism and Machine Theory*, 2012, vol. 143, p. 103622. DOI: 10.1016/j.mechmachtheory.2019.103622.
20. Dresig H., Vul'fson I.I. *Dynamik der mechanismen*. Wien, New York, Springer, 1989. 328 p. ISBN 978-3-7091-9036-4. DOI: 10.1007/978-3-7091-9035-7.
21. Frolov K.V. *Teoriya mekhanizmov i mashin* [Theory of mechanisms and machines]. Moscow, Vysshaya shkola Publ., 1987. 496 p.
22. Vul'fson I. *Dynamics of cyclic machines*. Cham, Springer International, 2015. 390 p. ISBN 978-3-319-12633-3. DOI: 10.1007/978-3-319-12634-0.
23. Artobolevskii I.I. *Teoriya mekhanizmov i mashin: uchebnyy dlya vtuzov* [Theory of mechanisms and machines]. 4th ed. Moscow, Nauka Publ., 1988. 640 p. ISBN 5-02-013810-X.
24. Rothbart H.A. *Cam design handbook*. New York, McGraw-Hill Professional, 2003. 606 p. ISBN 0071377573. ISBN 978-0875841830.
25. Faxin L., Xianzhang F. The design of parallel combination for cam mechanism. *Procedia Environmental Sciences*, 2011, vol. 10, pt. B, pp. 1343–1349. DOI: 10.1016/j.proenv.2011.09.215.
26. Sateesh N., Rao C.S.P., Janardhan Reddy T.A. Optimisation of cam-follower motion using B-splines. *International Journal of Computer Integrated Manufacturing*, 2009, vol. 22 (6), pp. 515–523. DOI: 10.1080/09511920802546814.
27. Myszka D.H. *Machines & mechanisms: applied kinematic analysis*. 4th ed. Upper Saddle River, NJ, Pearson, 2012. 376 p. ISBN 0132157802. ISBN 978-0132157803.



28. Varbanov H., Yankova T., Kulev K., Lilov S. S&A – Expert system for planar mechanisms design. *Expert Systems with Applications*, 2006, vol. 31 (3), pp. 558–569. DOI: 10.1016/j.eswa.2005.09.081.
29. Ondrášek J. The synthesis of a hook drive cam mechanism. *Procedia Engineering*, 2014, vol. 92, pp. 320–329. DOI: 10.1016/j.proeng.2014.12.129.
30. Mott R.L. *Machine elements in mechanical design*. 5th ed. Upper Saddle River, NJ, Pearson, 2013. 816 p. ISBN 0135077931. ISBN 978-0135077931.
31. Zhoua C., Hua B., Chen S., Mac L. Design and analysis of high-speed cam mechanism using Fourier series. *Mechanism and Machine Theory*, 2016, vol. 104, pp. 118–129. DOI: 10.1016/j.mechmachtheory.2016.05.009.
32. Tir K.V. *Kompleksnyi raschet kulachkovykh mekhanizmov* [Complex calculation of cam mechanisms]. Moscow, Mashgiv Publ., 1958. 380 p.
33. Podgorniy Yu.I., Skeebe V.Yu., Martynova T.G., Pechorkina N.S., Skeebe P.Yu. Kinematic analysis of crank-cam mechanism of process equipment. *IOP Conference Series: Materials Science and Engineering*, 2018, vol. 327, p. 042080. DOI: 10.1088/1757-899X/327/4/042080.
34. Podgorniy Yu.I., Skeebe V.Yu., Kirillov A.V., Maksimchuk O.V., Skeebe P.Yu. Proektirovanie kulachkovogo mekhanizma s uchetom tekhnologicheskoi nagruzki i energeticheskikh zatrat [Cam mechanism designing with account of the technological load and energy costs]. *Obrabotka metallov (tekhnologiya, oborudovanie, instrumenty) = Metal Working and Material Science*, 2017, no. 2 (75), pp. 17–27. DOI: 10.17212/1994-6309-2017-2-17-27.
35. Podgorniy Yu.I., Skeebe V.Yu., Kirillov A.V., Martynova T.G., Skeebe P.Yu. Motion laws synthesis for cam mechanisms with multiple follower displacement. *IOP Conference Series: Materials Science and Engineering*, 2018, vol. 327, p. 042079. DOI: 10.1088/1757-899X/327/4/042079.
36. Fialkova E.A. *Gomogenizatsiya. Novyi vzglyad* [Homogenization. A new look]. St. Petersburg, GIORD Publ., 2006. 386 p. ISBN 5-98879-032-1.
37. Panfilov V.A., ed. *Mashiny i apparaty pishchevykh proizvodstv*. V 2 kn. Kn. 1 [Machines and apparatus for food production. In 2 bk. Bk. 1]. Moscow, Vysshaya shkola Publ., 2001. 703 p. ISBN 5-06-004168-9.
38. Fomin A., Paramonov M. Synthesis of the four-bar double-constraint mechanisms by the application of the Grubler's method. *Procedia Engineering*, 2016, vol. 150, pp. 871–877. DOI: 10.1016/j.proeng.2016.07.034.
39. Fomin A., Dvornikov L., Paramonov M., Jahr A. To the theory of mechanisms subfamilies. *IOP Conference Series: Materials Science and Engineering*, 2016, vol. 124, p. 012055. DOI: 10.1088/1757-899X/124/1/012055.
40. Neklyutin D.A. *Optimal'noe proektirovanie kulachkovykh mekhanizmov na EVM* [Optimal design of cam mechanisms on a computer]. Moscow, Almata Publ., 1977. 215 p.
41. Tartakovskii I.I. Nekotorye zadachi sinteza optimal'nykh zakonov dvizheniya [Some problems of synthesis of optimal laws of motion]. *Mashinostroenie = Mechanical Engineering*, 1971, no. 2, pp. 39–43.

## Conflicts of Interest

The authors declare no conflict of interest.

© 2025 The Authors. Published by Novosibirsk State Technical University. This is an open access article under the CC BY license (<http://creativecommons.org/licenses/by/4.0>).